ONERA M6 Wing Data and CFD Results

David P. Young and Dmitri S. Kamenetskiy
The Boeing Company

Abstract

We present state of the art CFD code results for the ONERA M6 wing test case and a typical commercial airplane high lift configuration that document early separation, a common phenomenon when using typical RANS turbulence models. In at least some cases, properly stabilized integral boundary layer models using sweep and taper assumptions do not show the early stall phenomena. More research is needed to determine the strengths and weaknesses of various RANS methodologies and models (Drela's strip IBL is also based on the RANS assumptions).

1 Introduction

The ONERA M6 wing is a classic test case for CFD. There were two test campaigns with this wind tunnel model. The more widely known one is documented in [1] and this is the test data we use in this report. A recently discovered earlier test is documented in [2]. The airfoil sections have no camber and there is very little aft loading. Generally, the viscous effects are not very important up to the onset of massive separation. Based on a visual inspection of the graphics in [7], we could not find any qualitative differences between the two sets of data for the lowest angle of attack. It would be interesting to compare the two data sets for all the alphas and flight conditions. Mayeur et. al. [7] also developed a sharp trailing edge geometry and compared RANS solutions to those for the blunt trailing edge geometry that was tested. For the lower alpha considered, there are very minimal differences in pressure distributions. There were several papers discussing CFD solutions for the ONERA M6 wing in the late 1980's and early 1990's. The work of Rumsey and Vatsa [6] also found substantial differences between turbulence models popular at that time. The excellent work of Lee-Rausch et. al. [9] is a recent contribution of interest.

2 CFD codes

This test case has been run in TRANAIR, a full potential inviscid solver coupled with Drela's integral boundary layer with sweep and taper approximations. We also employed the Zeus system built around the RANS code CFL3D using the grid from the NASA website. It was found that at the higher alphas CFL3D convergence was vastly better with the thin layer option for the viscous terms. With full Navier Stokes, inconsistent levels of residual convergence were obtained. While the NASA grid is rather coarse, we also used the GGNS RANS solver with the SA turbulence model. A series of solution adaptive grids generated with the EPIC package was used. We believe the GGNS solutions presented here are essentially grid converged. The separation pattern remained largely unchanged from the CFL3D results. Numerous other sources document that RANS seems to suffer from early onset of separation for this case at least with the common eddy viscosity turbulence models. DLR [8] documents leading edge separation at $\alpha = 4.08$. However, as reported in [9], this could not be replicated with finer grids. Our results, also show no such separation at this angle of attack. At the higher alphas however, we did find far outboard leading edge separation. In our results, the behaviour appears to be rather insensitive to various corrections to the models such as the RC correction for the SA model and to the QCR constitutive relation correction.

M_∞	α	Reynolds number
0.8395	3.06	11.72 million
0.8358	4.08	11.81 million
0.8447	5.06	11.78 million
0.8372	6.06	11.71 million

Table 1: Reported Test Conditions for Considered Runs.

3 Results

Here we focus on the test runs with $M_\infty \simeq 0.84$. Table 1 gives the conditions reported for the four wind tunnel runs we focus on here.

In Figures 1, 2, 3, 4, 5, 6, 7, and 8, we show the sectional comparisons for these four conditions. All were run in the CFD codes with $M_\infty = 0.84$ and Reynold's number equal to 11.72 million per mean aerodynamic chord. In Figures 9, and 10, the results are shown for another run with $M_\infty = 0.6971, \alpha = 6.08$. The Reynolds' number for this run was reported as 11.74 million. TRANAIR's shocks are somewhat too far aft for some of the sections reported here but overall the test data seems to be rather well predicted. Rumsey [10] reports similar separation patterns on the outboard wing at $\alpha = 5.06$ in his own partially converged simulations with SA, SST and a Reynolds Stress Model.

Subsequently, GGNS was used in conjunction with EPIC and two different error metrics for grid adaptivity to generate two grid converged solutions for the $\alpha = 5.06$ case. Sectional cuts of these solutions are shown in Figures 14, and 15.

This test data has been criticized because of the tunnel mounting system. The good agreement of TRANAIR with the data would tend to support the idea that the mounting system has little effect on the outboard wing. Mayeur et. al. state that the Gousse [2] test set up would have been expected to minimize tunnel wall effects at the root of the wing. It would be interesting to access this data as well. Gerard Carrier [11] stated that the two tests resulted in consistent pressure data.

3.1 777-200 Flaps 30 Simulations

Another case examined is the 777-300 with flaps deployed at setting 30. The results shown here were reported in [12]. There is some flow separation at most angles of attack. standard BCA processes for unstructured gridding and CFD solution were used. The grid had about 112 million total elements comprised of prisms and tetrahedrons. Of note for this case is the early stall of the CFD simulations compared to test data. For BCFD, all runs were started from freestream, while for CFD++ and GGNS, angles of attack higher than 14 were started from the next lower value of α in an attempt to prevent premature stall. In Figure 16 we show the $C_L - \alpha$ curves, the pitching moment data, and the drag polars. Note that a single square on the drag axis is 2000 counts of drag.

4 Conclusions

We suggest that this study is an indication that RANS can suffer from premature separation. This behavior is seen on both coarse grids and essentially grid converged solution adaptive grids. In the case of the ONERA M6, IBL seems to hold together and predict reasonable pressure distributions. This premature stall is also seen for the high lift 777-200 configuration.

We can theorize as to why RANS appears to be ill-posed in separated flow. The Euler equations can be reformulated to show that the total pressure and total temperature are constant on streamlines. Thus if there is a closed streamline (as often happens in separated flows) the equations will be singular. Some regularization inevitably involving viscosity will be required. With the Navier-Stokes equations there is the molecular viscosity term which in principle could make the system well posed. However, as the Reynolds' number increases this becomes problematic numerically. When the viscous terms are 6 or 7 orders of magnitude smaller than the convective terms as is often the case in aeronautical flows, grid sizes needed to reduce numerical viscosity to levels below the viscous terms will be very small. The same can be true of the eddy viscosity at least far from the wall. Thus, RANS will be quite sensitive to the exact level of grid in separated flow regions.

Some might conclude from this that the future of CFD lies with time accurate eddy resolving simulations. The authors disagree. There are a host of well known issues that will continue to plague these costly simulations, barring some fundamental theoretical breakthrough.

Any turbulent time accurate eddy resolving simulation will show chaotic behavior and will be ill posed as an initial value problem [14, 15]. Pointwise errors will grow exponentially as the system is integrated in time. There is no single "right" answer and the results are best described by a probability distribution.

"At least there is an attractor" is the best honest argument for these simulations. However, attractor dimension is unknown. Best bounds are large. More importantly, Lyopunov constants are unknown. Thus we don't know how "attractive" the attractor is. Strong "attractiveness" may be required if simulations are going to be skillful. "Attractiveness" must overcome perhaps large and uncontrollable by classical methods numerical errors. There will be saddle and bifurcation points. There can be many many branches at such a point.

Because of the ill-posedness of the initial value problem, the adjoint diverges and classical methods of numerical error control fail. Thus, it becomes very problematic to try to separate numerical from model error. In this situation, standard methods of code and model verification and validation are not really applicable. This is a selection bias machine and people find it easy to fool themselves [13].

At least with steady state simulations, it is often possible to determine things like bifurcation points, multiple solutions, stability to perturbations and achieve grid and residual convergence. Much better strong solver methods will be needed to do all this. GGNS is a big step forward in solver technology and is superior to that in TRANAIR. TRANAIR had to take shortcuts because of computer limitations in the 1980's.

Further, there are issues with RANS that need to be addressed. An example is the numerical issues with SST at the wall. QCR2020 is an example of how RANS can be improved. It is almost certainly true that RANS can be improved, perhaps dramatically improved. Excessive focus on more and more "frameworks" for "running (flawed) codes", "getting the right answer", and soft money capture point the field in the wrong direction. Real progress must be preceded by an honest assessment of the defects in current CFD.

References

[1] V. Schmitt and F. Charpin, "Pressure Distributions on the ONERA-M6-Wing at Transonic Mach Numbers," Experimental Data Base for Computer Program Assessment, AGARD Advisory Report AR-138, May 1979.

[2] M. Gousse, "Etude de l'coulement autour de l'aile M6 S1MA,", ONERA internal report, Feb. 1979.

[3] V. N. Vatsa, "Accurate Numerical Solutions for Transonic Viscous Flow over Finite Wings," Journal of Aircraft, Vol. 24, No. 6, June 1987, pp. 377-385.

[4] R. Abid, V. N. Vatsa, D. A. Johnson and B. W. Wedan, "Prediction of Separated Transonic Wing Flows with a Non-Equilibrium Algebraic Model," AIAA 27th Aerospace Sciences Meeting, AIAA Paper 1989-0558, Jan. 1989.

[5] R. Radespiel, C. Rossow, and R. C. Swanson, "An Efficient Cell-Vertex Multigrid Scheme for the Three-Dimensional Navier-Stokes Equations," AIAA Ninth Computational Fluid Dynamics Conference, AIAA Paper 1989-1953, June 1989.

[6] C. L. Rumsey and V. N. Vatsa, "Comparison of the Predictive Capabilities of Several Turbulence Models Viscous Flow over Finite Wings," Journal of Aircraft, Vol. 32, No. 3, May-June 1995, pp. 510-514.

[7] L. Mayeur, A. Dumont, D. Destarac, and V. Gleize, "RANS Simulations on TMR 3D Test Cases with the Onera elsA Flow Solver," 54th AIAA Aerospace Sciences Meeting, San Diego, California, AIAA 2016-1357.

[8] N. Kroll and C. Rossow, "Digital-X: DLR's Way Towards the Virtual Aircraft", NIA CFD Conference on Future Directions in CFD Research, A Modeling and Simulation Conference, Hampton, Virginia, August, 2012.

[9] E. M. Lee-Rausch, C. L. Rumsey, and B. Eisfeld, "Application of a Full Reynolds Stress Model to High Lift Flows", AIAA 2016-3944, 46th AIAA Fluid Dynamics Conference, 13-17 June, 2016, Washington DC, USA.

[10] Private communication, Christopher Rumsey, November 2016.

[11] Private communication, Gerard Carrier, November 2016.

[12] J. E. Bussoletti, D. E. Williams, D. S. Kamenetskiy and V. Venkatakrishnan, "Fixed Grid Unstructured Grid Study – A Comparison of CFD++, BCFD, and GGNS Solvers for a Variety of Test Cases," Boeing Coordination Sheet Tech-B-BBA5-C2015-006, 2015.

[13] E. N. Lorenz, "Deterministic Nonperiodic Flow", *Journal of Atmospheric Sciences*, Vol. 20, pp. 130–141, 1963.

[14] J. Slingo and T. Palmer, "Uncertainty in Weather and Climate Prediction," *Philosophical Transactions of the Royal Society A*, 13 December, 2011.

[15] D. Sarewitz, "Beware the creeping cracks of bias," *Nature*, Vol. 485, Issue 7397, 10 May, 2012.

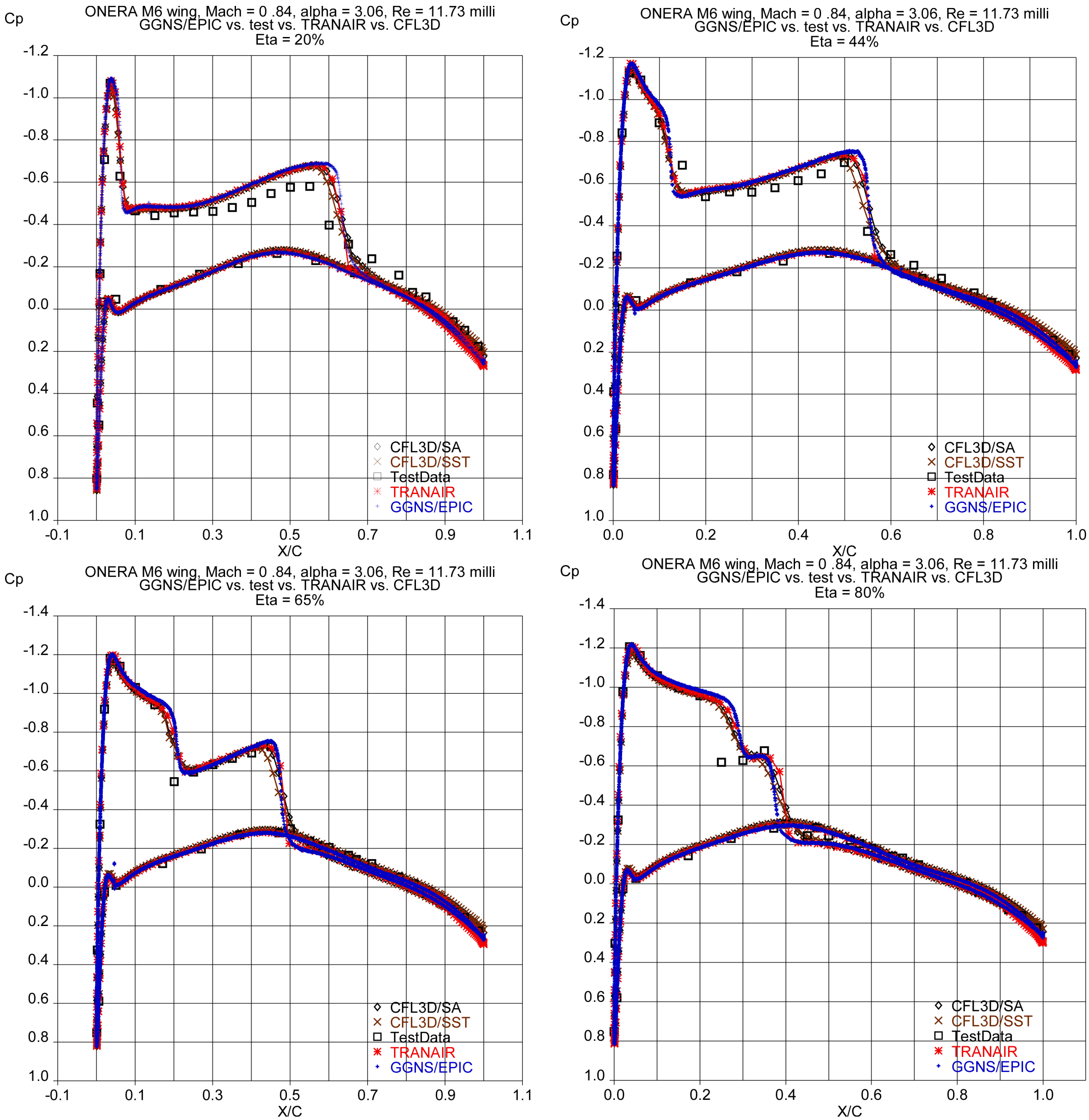

Figure 1: Pressure Distributions for the ONERA M6 wing, $M_\infty = 0.84, \alpha = 3.06$.

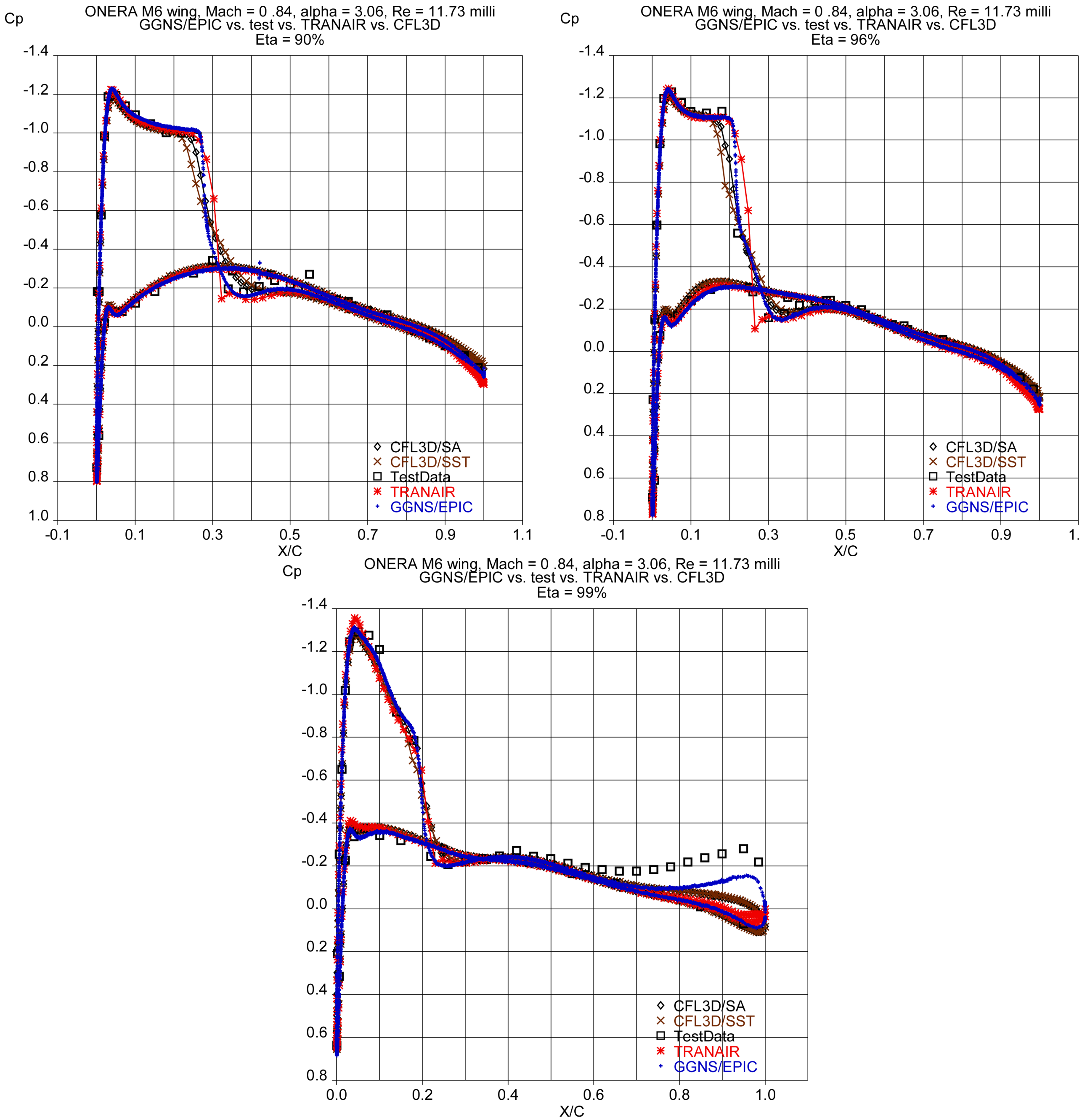

Figure 2: Pressure Distributions for the ONERA M6 wing, $M_\infty = 0.84, \alpha = 3.06$.

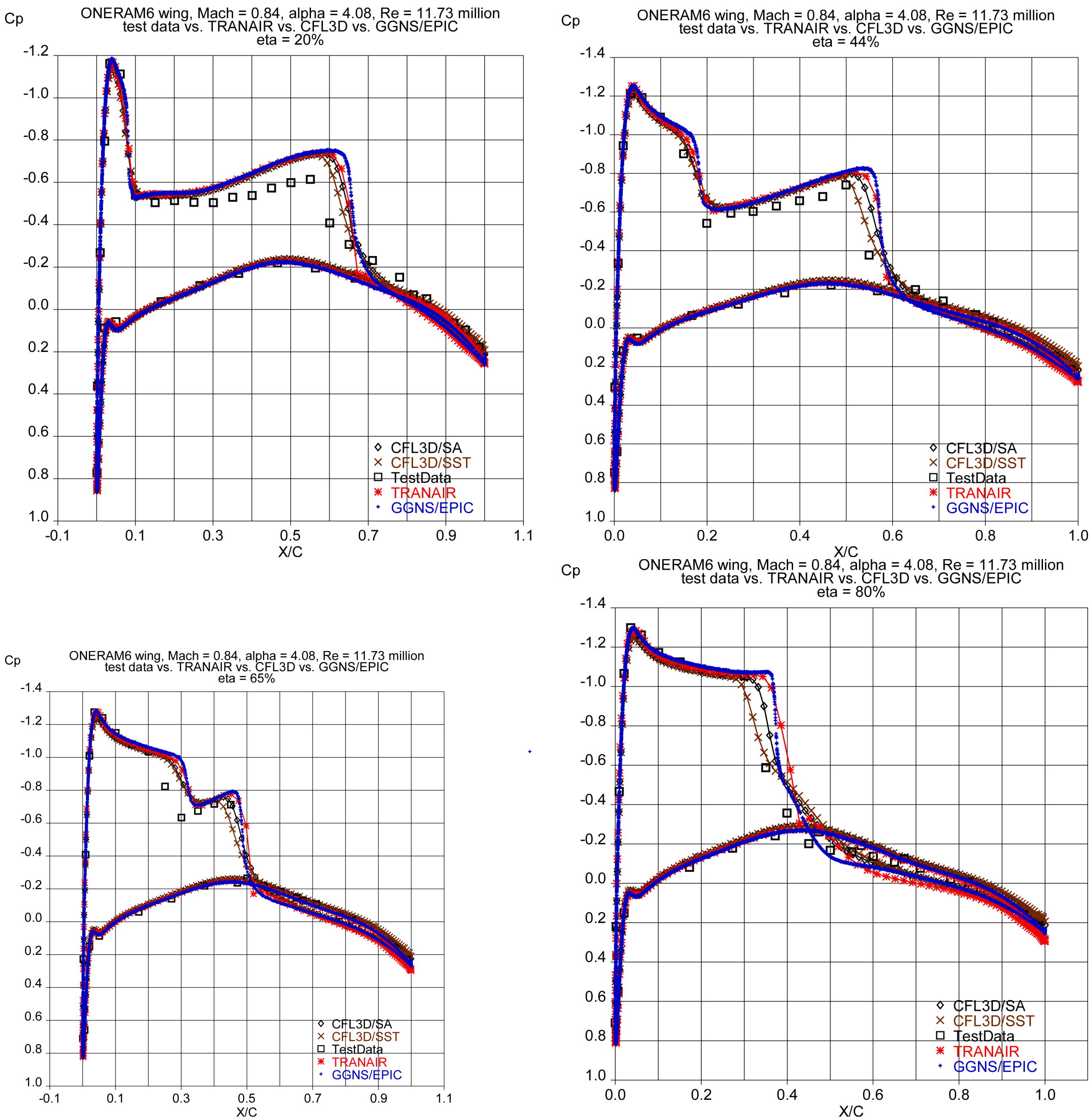

Figure 3: Pressure Distributions for the ONERA M6 wing, $M_\infty = 0.84, \alpha = 4.08$.

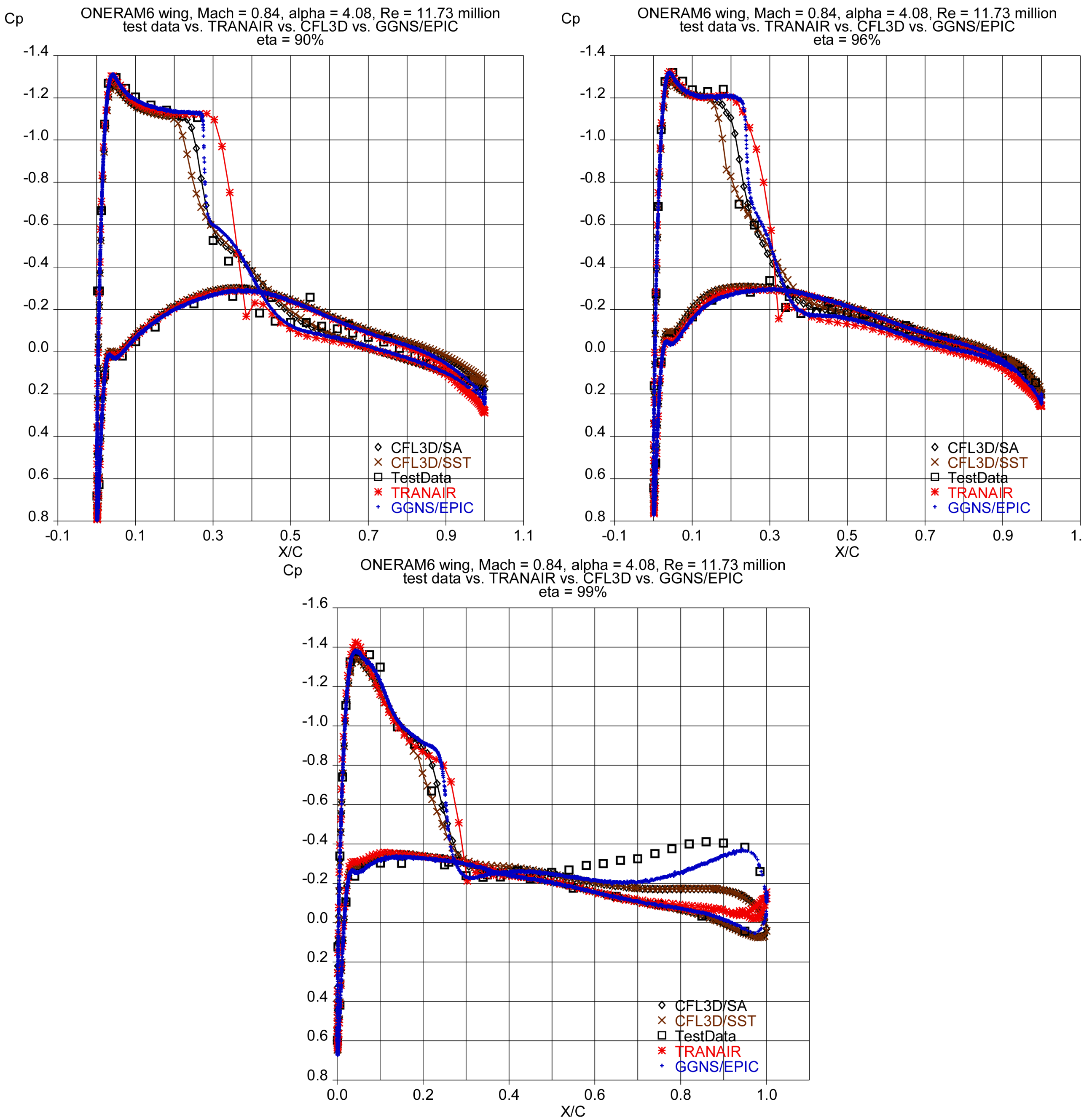

Figure 4: Pressure Distributions for the ONERA M6 wing, $M_\infty = 0.84, \alpha = 4.08$.

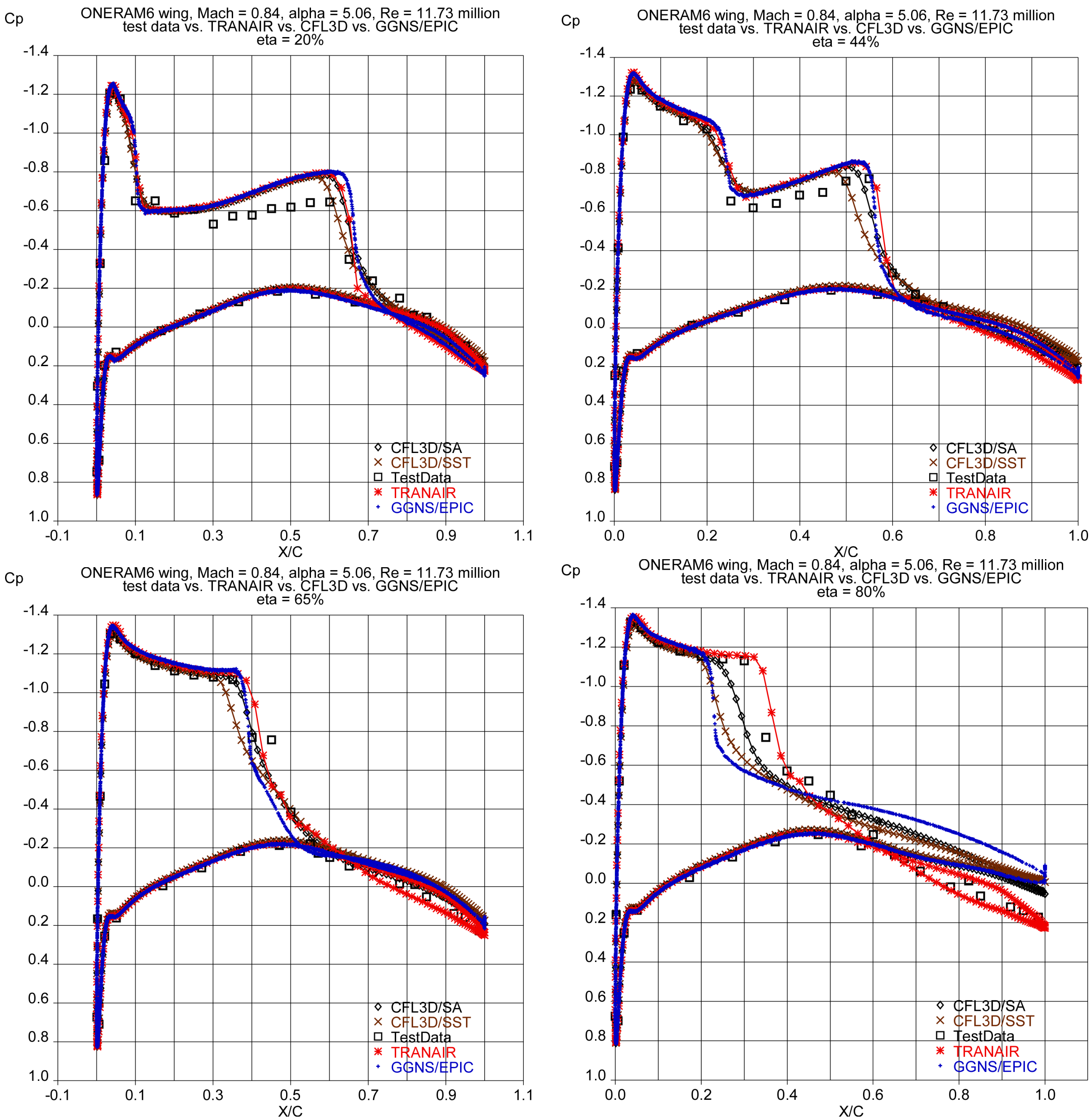

Figure 5: Pressure Distributions for the ONERA M6 wing, $M_\infty = 0.84, \alpha = 5.06$.

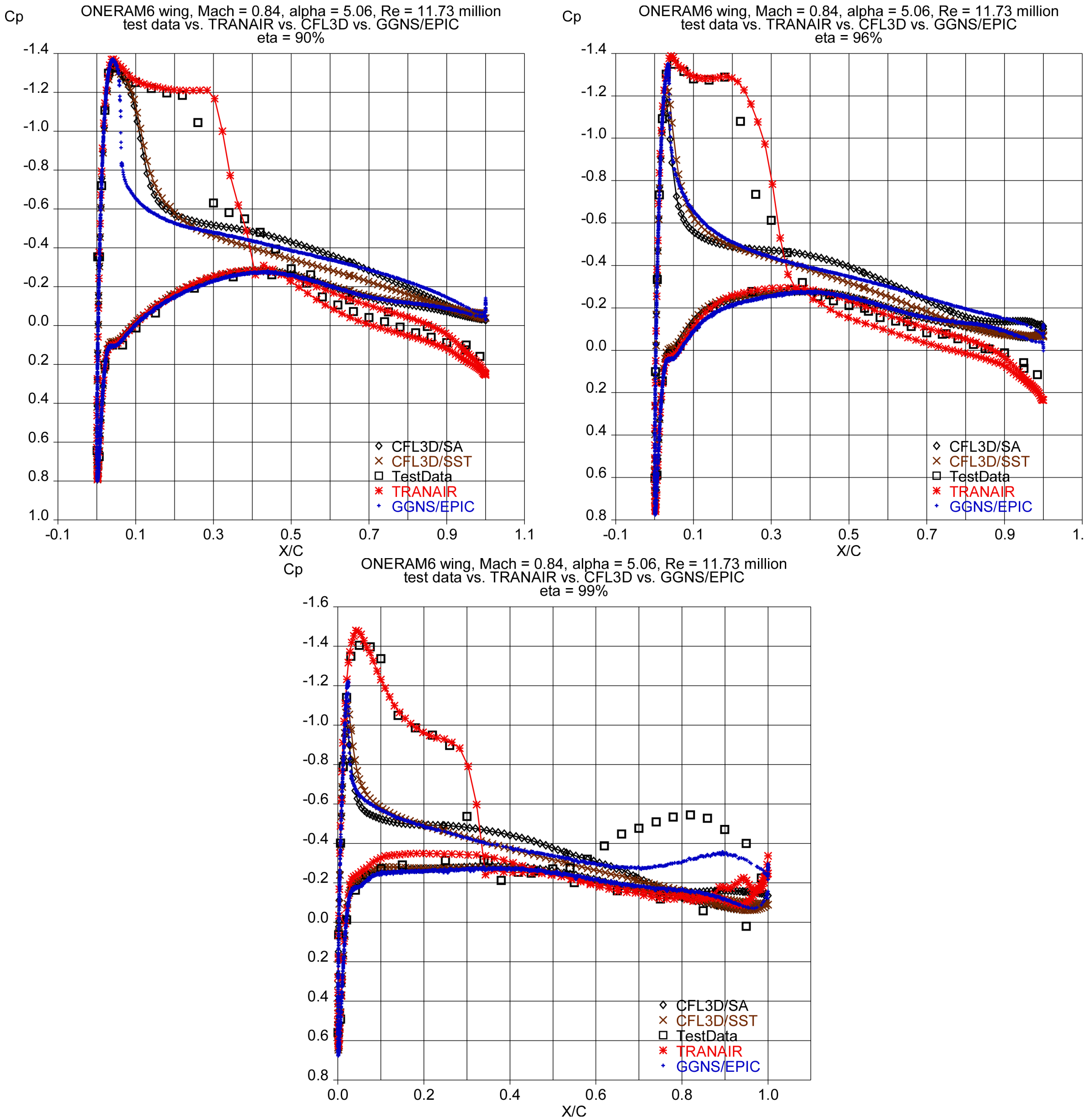

Figure 6: Pressure Distributions for the ONERA M6 wing, $M_\infty = 0.84, \alpha = 5.06$.

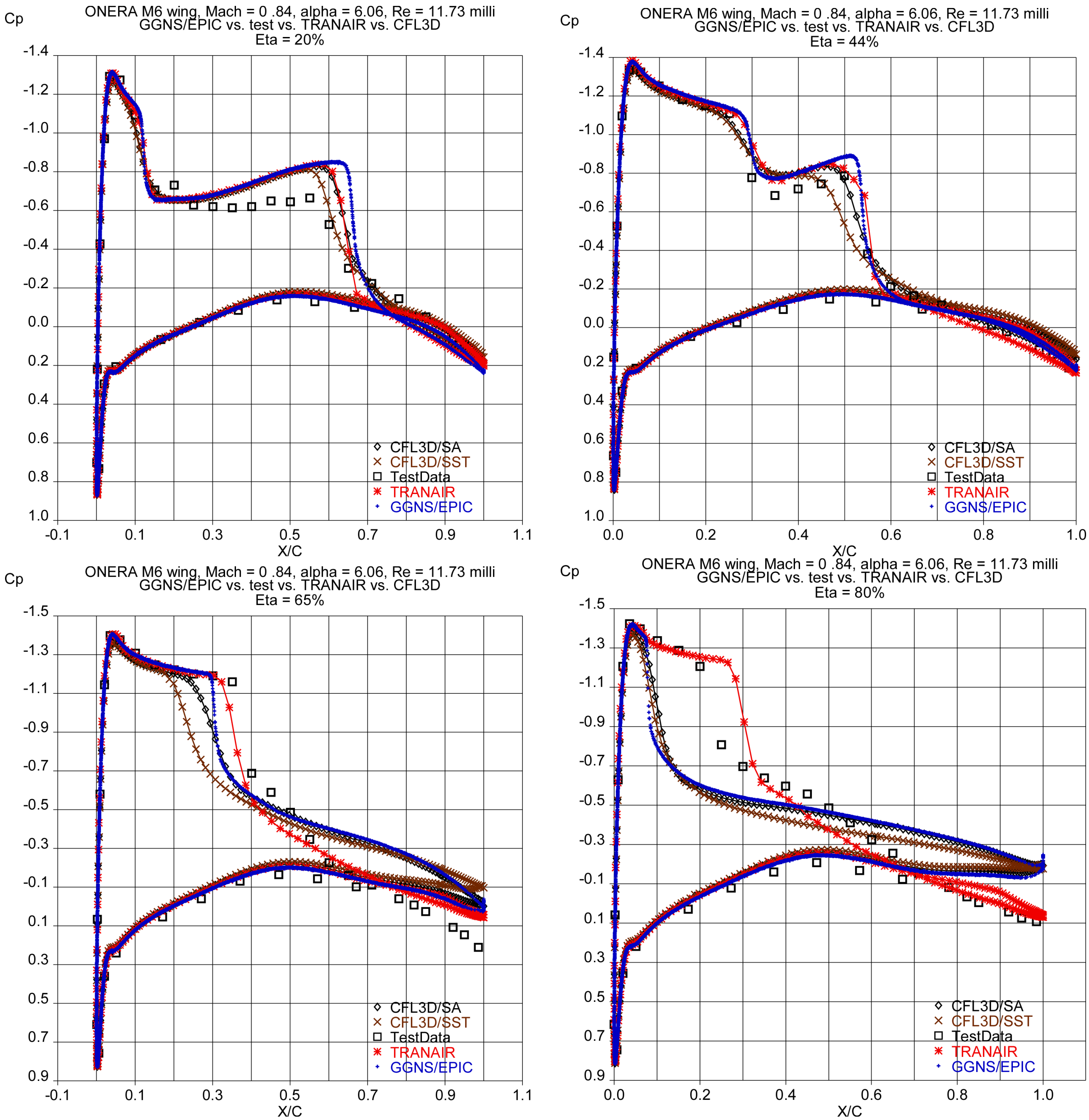

Figure 7: Pressure Distributions for the ONERA M6 wing, $M_\infty = 0.84, \alpha = 6.06$.

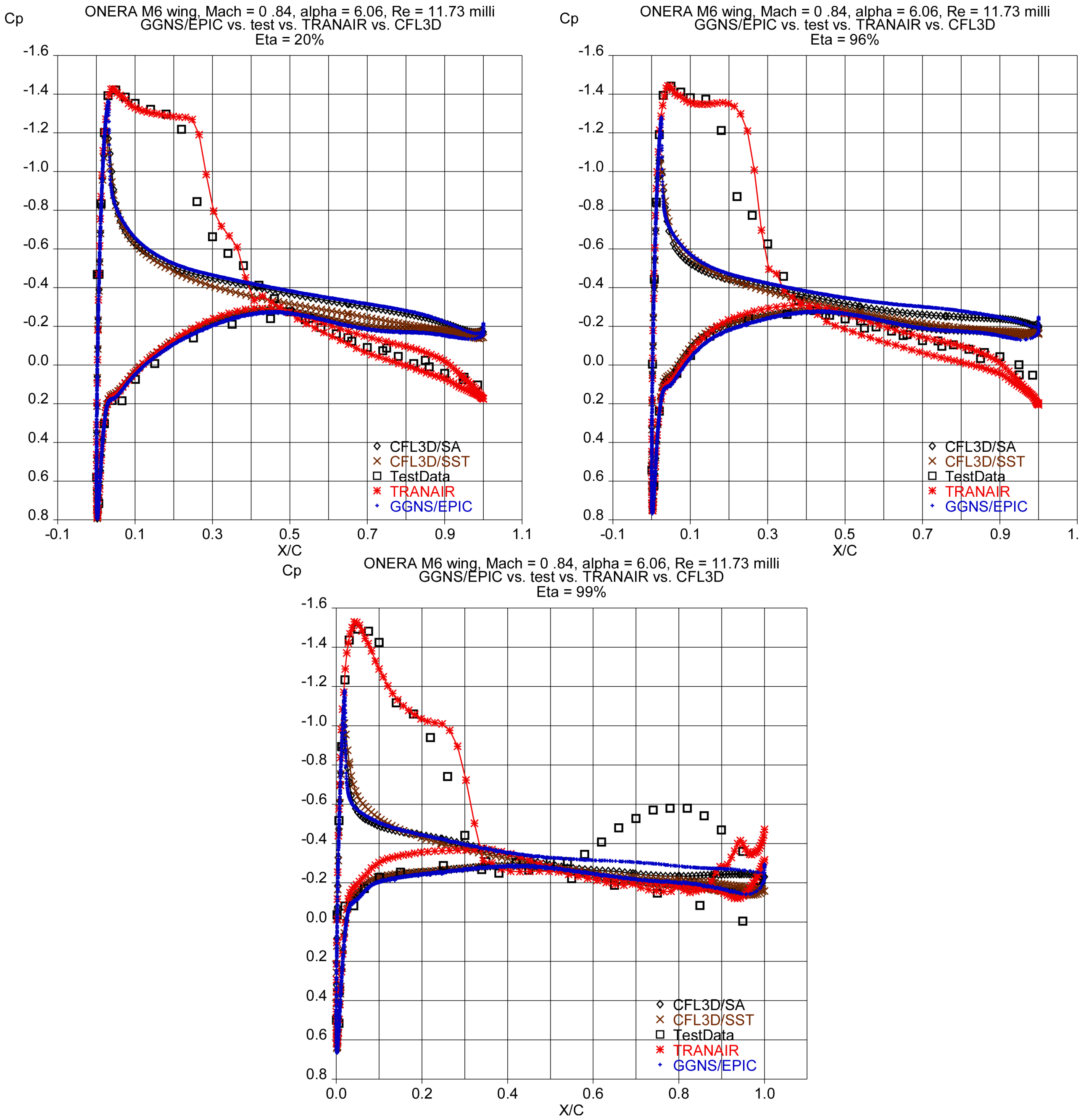

Figure 8: Pressure Distributions for the ONERA M6 wing, $M_\infty = 0.84, \alpha = 6.06$.

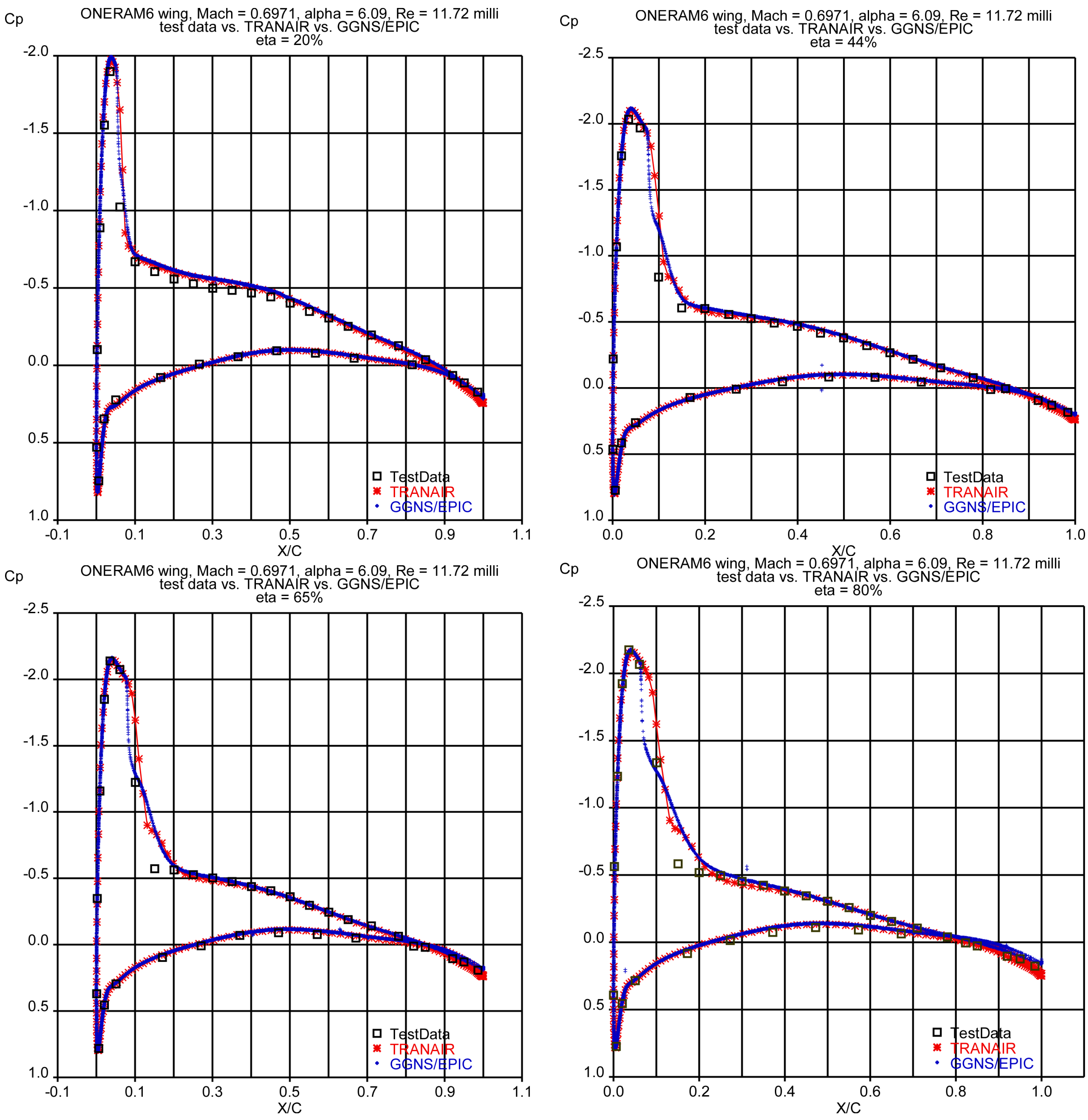

Figure 9: Pressure Distributions for the ONERA M6 wing, $M_\infty = 0.6971, \alpha = 6.09$.

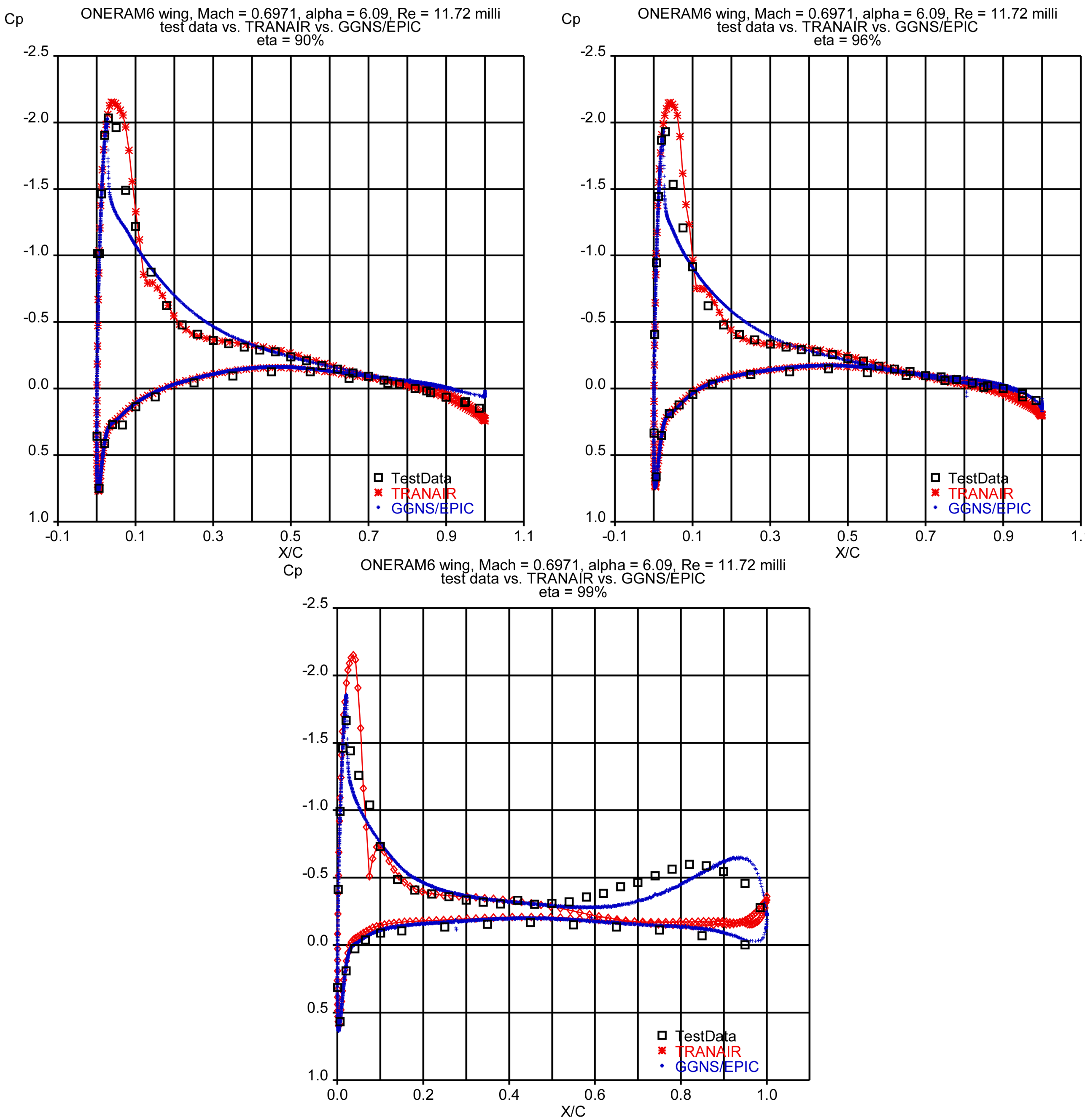

Figure 10: Pressure Distributions for the ONERA M6 wing, $M_\infty = 0.6971, \alpha = 6.09$.

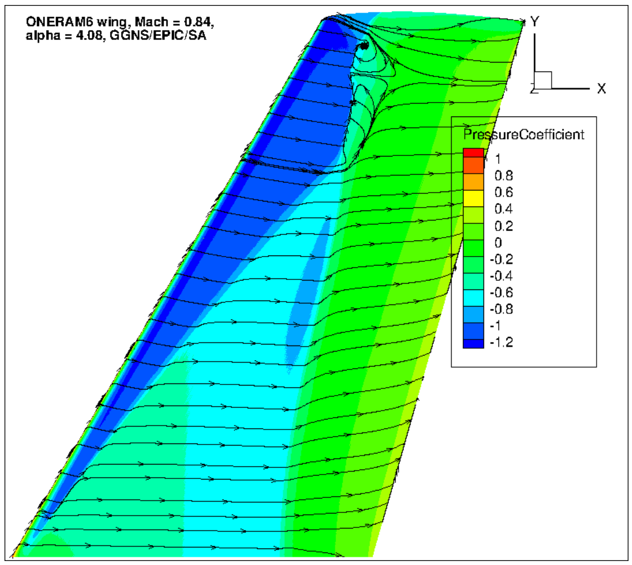

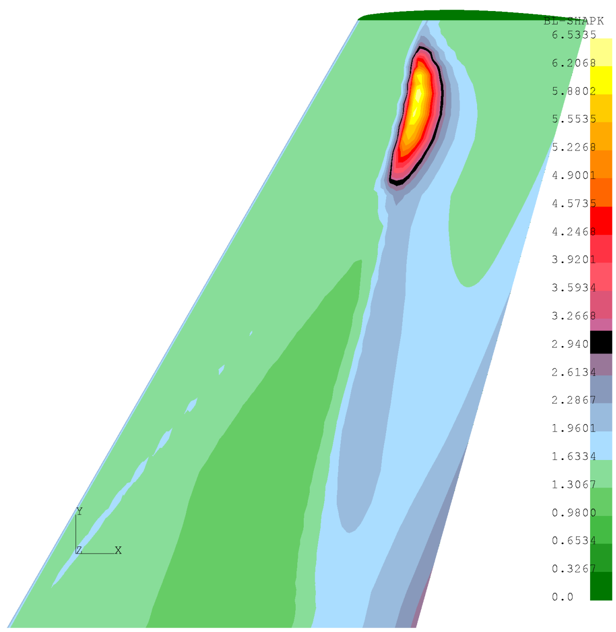

Figure 11: Separation Patterns from GGNS/EPIC and TRANAIR for the ONERA M6 wing, $M_\infty = 0.84, \alpha = 4.08$.

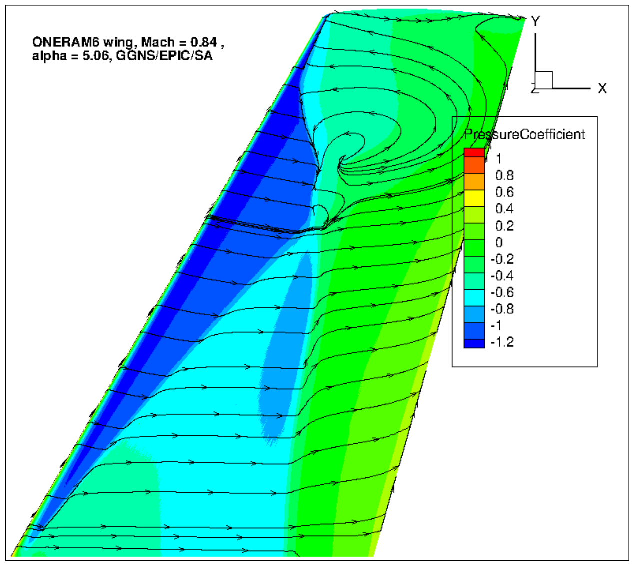

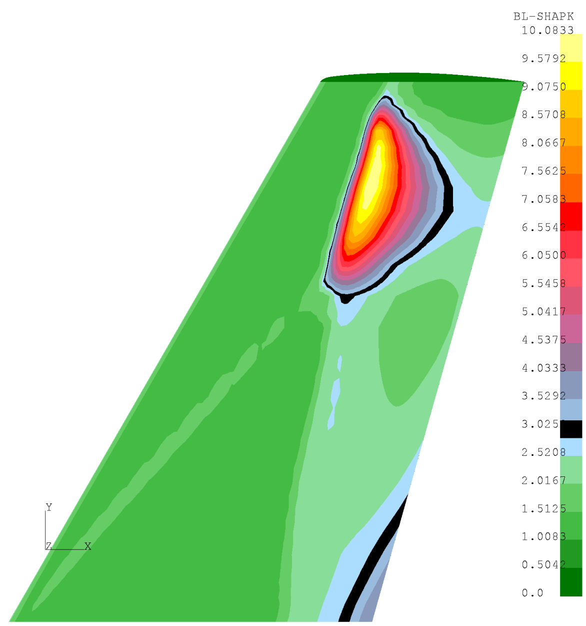

Figure 12: Separation Patterns from GGNS/EPIC and TRANAIR for the ONERA M6 wing, $M_\infty = 0.84, \alpha = 5.06$.

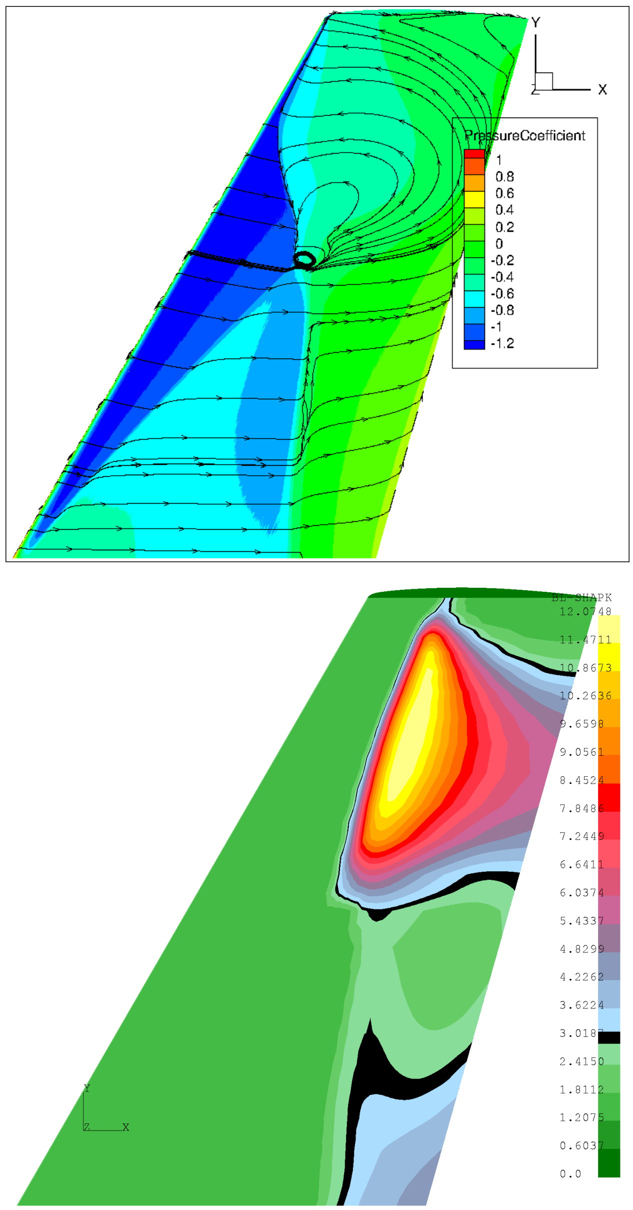

Figure 13: Separation Patterns from GGNS/EPIC and TRANAIR for the ONERA M6 wing, $M_\infty = 0.84, \alpha = 6.06$.

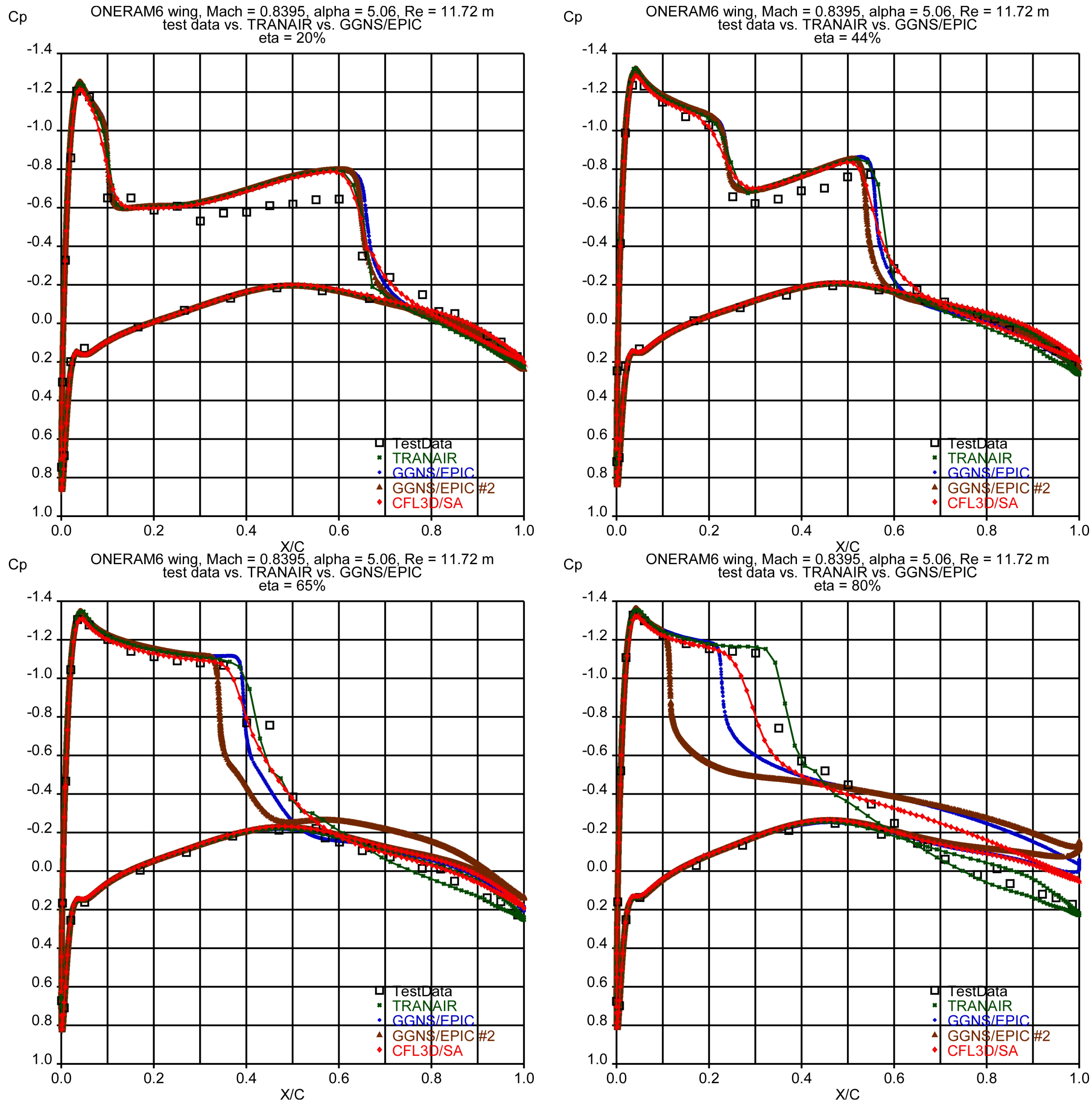

Figure 14: Pressure Distributions for the ONERA M6 wing, $M_\infty = 0.84, \alpha = 5.06$.

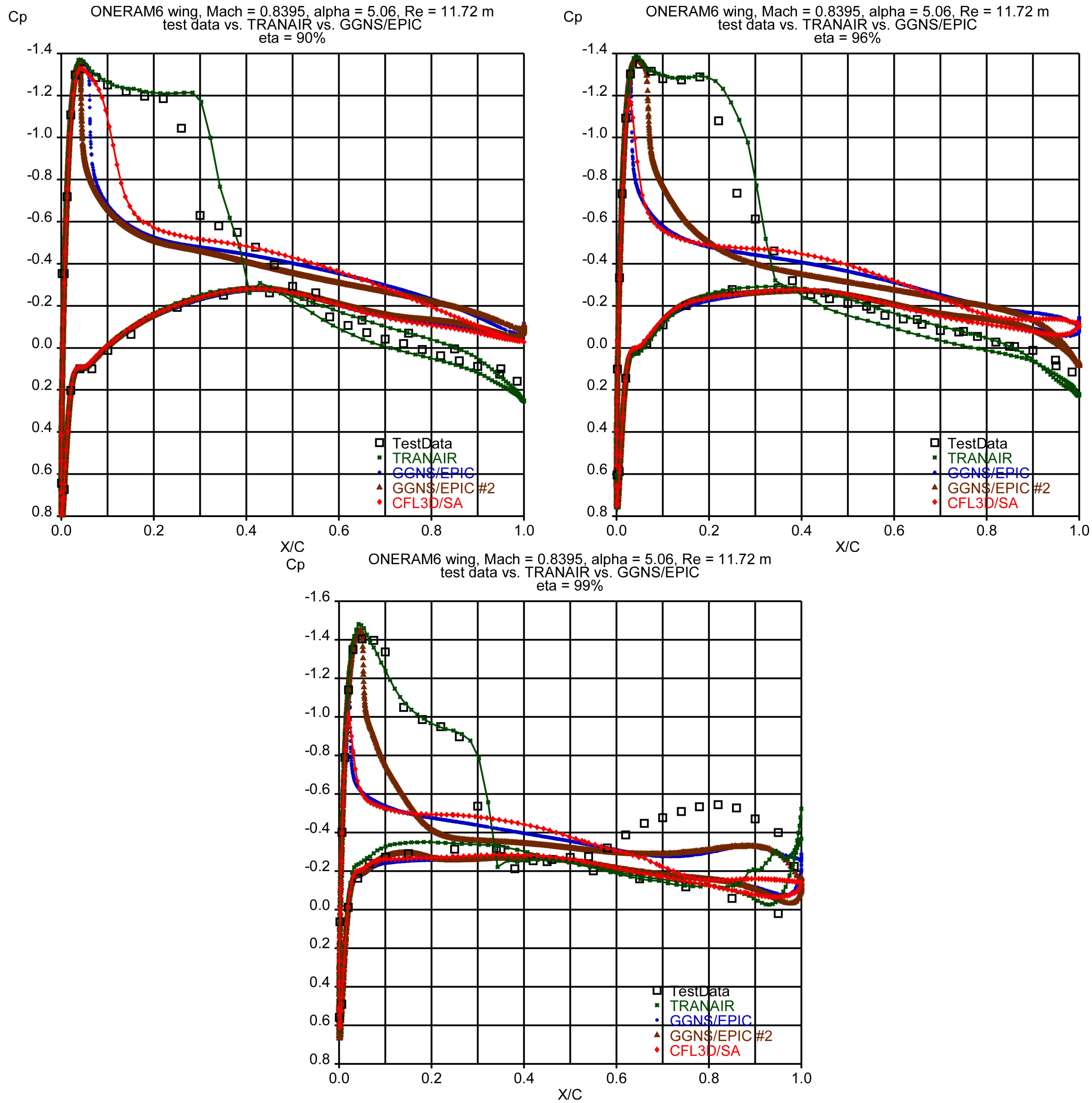

Figure 15: Pressure Distributions for the ONERA M6 wing, $M_\infty = 0.84, \alpha = 5.06$.

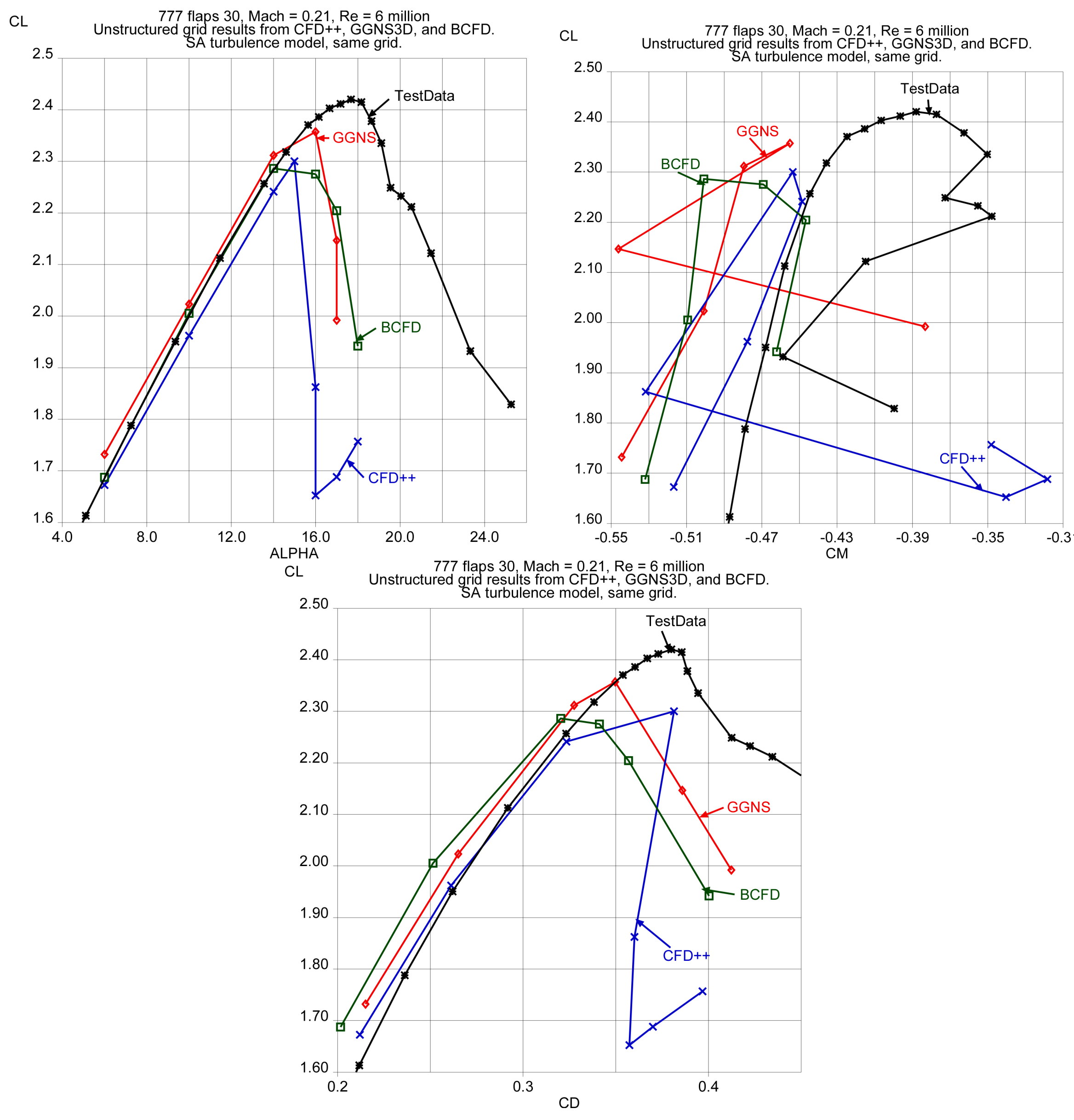

Figure 16: $C_L - \alpha$ Curves, $C_L - C_M$ Curves, and Drag Polars for the 777-200 Flaps30 Configuration using BCFD, CFD++, and GGNS and the Experimental Data.